Use of microseismicity for determining the structure of the fracture network of large-scale porous media

Tayeb A. Tafti,[1] Muhammad Sahimi,[1,*] Fred Aminzadeh,[1] and Charles G. Sammis[2]
[1]*Mork Family Department of Chemical Engineering and Materials Science, and the Petroleum Engineering Program, University of Southern California, Los Angeles, California 90089-1211, USA*
[2]*Department of Earth Sciences, University of Southern California, Los Angeles, California 90089, USA*
(Received 15 November 2012; published 25 March 2013)

We show that microseismic events—earthquakes with small magnitudes—can be fruitfully used to gain insight into the properties of the fracture network of large-scale porous media, such as oil, gas, and geothermal reservoirs. As an example, we analyze extensive data for the Geysers geothermal field in northeast California. Injection of cold water into the reservoir to produce steam leads to microseismic events. It is demonstrated that the analysis can also lead to insight into whether the fractures are of tectonic type or induced by injection of cold water. To demonstrate this we estimate, using the catalogue of the microseismic events, the fractal dimension D_f of the spatial distribution of hypocenters of the events in three seismic clusters associated with the injection of cold water into the field, as well as the b values in the Gutenberg-Richter frequency-magnitude distribution. The fractal dimensions are all in a narrow range centered around $D_f \simeq 2.57 \pm 0.06$, comparable to the measured fractal dimension of fracture sets in the greywacke reservoir rock. For most cases the b values are about $b \simeq 1.3 \pm 0.1$, consistent with the Aki relation, $D_f = 2b$. Both D_f and b are significantly higher than those commonly observed for regional tectonic seismicity or aftershock sequences for which $D_f \approx 2$ and $b \approx 1$ are typical. Our results do not imply that no tectonic triggering exists in the reservoir, but rather that the overpressure allows the activation of less favorably oriented fractures that produce an increase in both b and D_f. The estimate $D_f \approx 2$ for tectonic seismicity has been interpreted as indicating that most tectonic events occur on the subset of near-vertical faults—because they have lower normal stress—or that they occur on the *backbone* of the fracture and fault network, the multiply connected part of the network that enables finite shear strain. Our results lend support to the latter. The results that the entire fracture network, and not just its backbone, is active at the Geysers indicate that the seismicity is not a result of the triggered release of tectonic stress, but is induced by the release of local stress concentrations, driven by thermal contraction that is not constrained by friction. The possible implication for hydraulic fracturing—so-called *fracking*—is also briefly discussed.

DOI: 10.1103/PhysRevE.87.032152 PACS number(s): 64.60.ah, 91.30.Dk, 91.30.Px, 91.55.Jk

I. INTRODUCTION

The Geysers geothermal field (GGF) is located about 150 km north of San Francisco, California; see Fig. 1. The field contains a large number of wells, some of which are used for injecting cold water into the porous formation. When water comes into contact with the hot matrix, it evaporates, generating steam that is produced from a network of fractures in the crystalline rock. Some of the fractures are of natural tectonic type associated with the nearby boundary of the San Andreas fault plate. On the other hand, when a fluid (such as cold water) is injected into the (hot) rock at high pressure, it induces nucleation and propagation of some fracture, and also activates the less favorably oriented fractures. Due to very low permeability of the formation matrix of the GGF, the steam production depends on the presence of natural or induced fractures. Cost-effective production of the steam requires that the trajectories of the wells intersect the densely fractured regions. Hence, locating such regions is vital to the economics of power generation from the GGF. Injection of a fluid, such as cold water, into a porous formation also induces microseismic events [1]—earthquakes with small magnitudes—and the purpose of this paper is to show that such events can help one to map out the fracture network of the GGT, or any other large-scale porous formation in which such events occur. Various approaches have been already used to characterize the fracture network of the GGF, including geologic mapping [2,3], outcrop analysis [4], core analysis [5], and shear wave splitting [6-9].

Studies by several groups have suggested that the fracture network of rock formations may be self-similar and scale-invariant (for a comprehensive recent review, see Sahimi [10] and Bonnet *et al*. [11]), implying that, statistically, the fracture network appears the same over a range of length scales, and that long-range correlations, which are a fundamental feature of fractal structures, affect any phenomenon that may occur in the network. Such studies began in 1985 when the geologic and hydrologic framework at Yucca Mountain in Nevada was studied. Barton and Larsen [12] developed the so-called *pavement method*, whereby one clears a subplanar surface and maps the fracture surface, in order to measure its connectivity, trace length, density, and scaling, in addition to the orientation, surface roughness, and aperture. An important result of the Yucca Mountain study was that the fractured pavements had a scale-invariant structure, characterized by a fractal dimension D_f defined by

$$n(\ell) \propto \ell^{-D_f}, \tag{1}$$

*Author to whom all correspondence should be addressed: moe@usc.edu

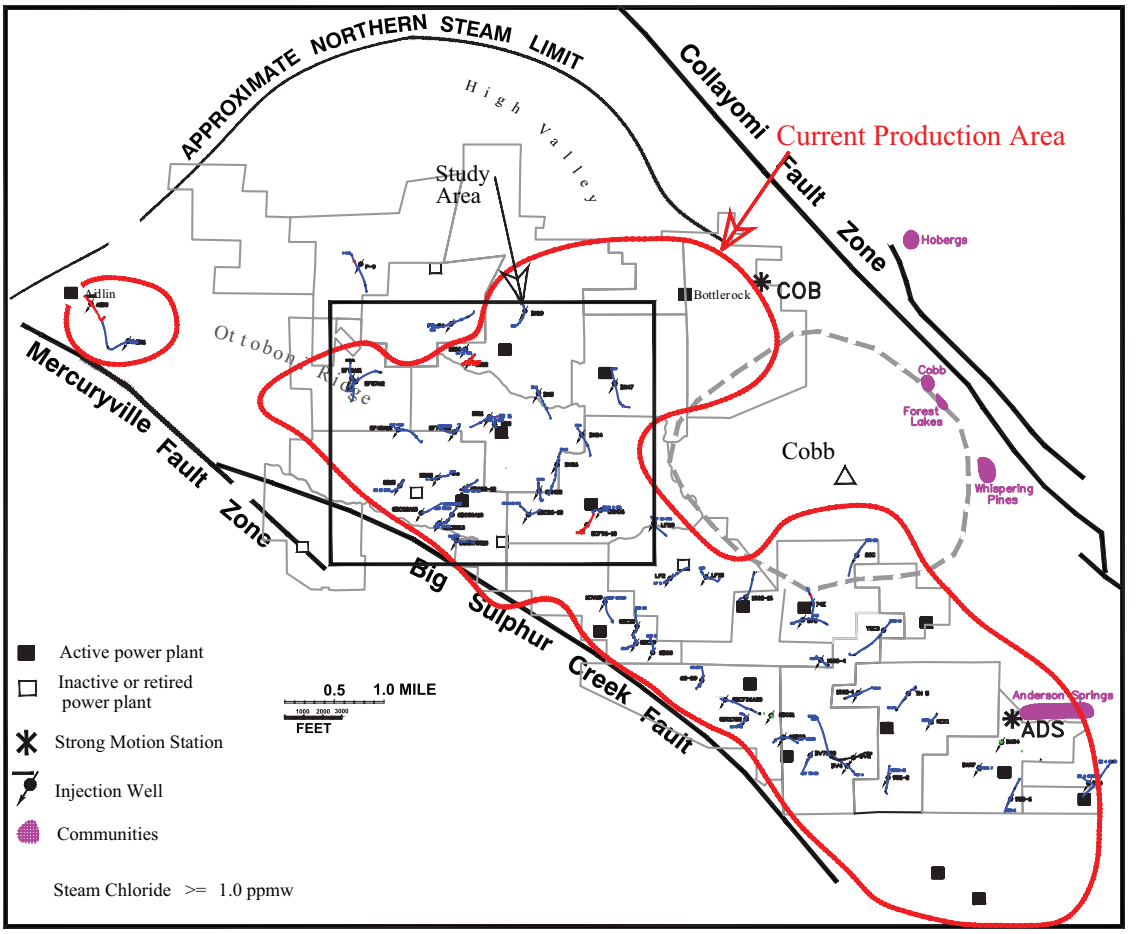

FIG. 1. (Color online) Map of the Geysers geothermal field, the area under study (in the rectangular area), and the locations of the injection wells and seismic activities.

where $n(\ell)$ is the number of fractures of length ℓ, and D_f is the fractal dimension of the network that is less than the Euclidean dimension of space in which the network is embedded. The Yucca Mountain study indicated that it is possible to represent the distribution of fractures ranging from 20 cm to 20 m by a single parameter, D_f. For the fracture surfaces analyzed by Barton and co-workers, $D_f \simeq 1.6$–1.7. LaPointe [13] carried out a careful reanalysis of three fracture-trace maps of Barton and Larsen [12] and estimated that the corresponding three-dimensional (3D) fracture networks are also fractal with $D_f \simeq 2.37$, 2.52, and 2.68. Velde *et al.* [14] analyzed the structure of fracture patterns in granites, while Vignes-Adler *et al.* [15] carried out the same type of analysis for fracturing in two African regions, and reported strong evidence for the fractality of the fracture patterns, while 2D maps of fracture traces spanning nearly ten orders of magnitude, ranging from microfractures in Archean Albites to large fractures in South Atlantic seafloors, were analyzed by Barton [16], who reported that $D_f \simeq 1.3$–1.7. Sammis *et al.* [17] analyzed the fracture pattern in the GGF over a wide range of scales, including regional maps, outcrops, and drill cores, and concluded that the fracture network in the greywacke reservoir rock has a fractal structure with a fractal dimension, as defined by Eq. (1), of $1.6 \leqslant D_f \leqslant 1.9$, in 2D (planar) sections. Sahimi *et al.* [18] suggested that the fractal dimensions of the fracture patterns in heterogeneous rock should be around 1.9 and 2.53 in two and three dimensions, respectively (see below). See also Hatton *et al.* [19] for further discussion of the issue of 2D and 3D sampling in laboratory tests. The results of such tests may depend on the heterogeneity and the anisotropy of the fracture set.

On the other hand, Hirata *et al.* [20] mapped the fault patterns in a certain rock formation and demonstrated that a fractal pattern should be expected from the fracturing process, generated by earthquakes of various sizes, and that the fractures generated are scale-invariant over multiple length scales, ranging from the microscopic to the field scale. Computer simulations in models of highly heterogeneous media [21-23], as well as simulation of hydraulic fracturing in which water is injected into a heterogeneous solid to generate fracture [24], indicated that the resulting fracture networks are self-similar fractals.

Since earthquakes usually occur on existing faults, the spatial pattern of their hypocenters is often used to gain insight into the structure of the underlying fault network. Hirata [25] estimated the fractal dimension of the spatial distribution of seismic events' hypocenters in the Tohoku region, based on a correlation function defined by [20]

$$C(r) = \frac{2}{N_t(N_t - 1)} N_r(R < r), \tag{2}$$

where $N_r(R < r)$ is the number of pairs of events that have a spacing R less than r, and N_t is the total number of events within the region of interest. As pointed out earlier, injection of high-pressure cold water into a geothermal reservoir induces microseismic events. Thus, if the spatial distribution of such microseismic events has a fractal structure, $C(r)$ should follow a power law,

$$C(r) \propto r^{D_f}. \tag{3}$$

The fractal dimension D_f defined by Eq. (3) is also called the *correlation dimension*, and denoted sometimes by D_c. Throughout this paper, whenever we refer to the fractal dimension of our own data, we mean D_f as defined by Eq. (3). Hirata [25] reported fractal dimensions between 1.34 and 1.79 in 2D sections. Robertson *et al.* [26] estimated the fractal dimension of the spatial distribution of the hypocenters of several aftershock sequences in south and central California, and reported D_f to be between 1.82 and 2.07 in three dimensions, with an average of about 1.95.

Aki [27] proposed an important relation between the fractal dimension D_f of a fault network and the b value in the Gutenberg-Richter (GR) law,

$$\log N(m > M) = a - bM, \tag{4}$$

with N being the number of events (earthquakes) with a magnitude greater than M. The GR law describes the magnitude-frequency distribution of seismicity that develops on the fault networks. If during an earthquake slip scales with the area of the active fault plane, then the Aki relation is given by $D_f = 3b/c$, where c is a scaling constant that has a world-wide average of about 1.5 [28]. But, whereas Hirata *et al.* [20] did not observe a correlation between the two for acoustic emissions in laboratory experiments, Hirata [25] reported the approximate relation $D_f \simeq 2.3 - 0.73b$ for seismicity in the Tohoku region in Japan. Comprehensive discussions of the relation between D_f and the b values are given by Wyss *et al.* [29] and Chen *et al.* [30].

In this paper, we report on our study of the use of microseismicity to deduce the structure of the fracture network of the GGF. We show that, in addition to characterization of the fracture network, the fractal dimension D_f of the network and its correlation with the b values enable one to understand the origin of the fracture network that exists in the rock formation. In addition, we address the question of whether the Aki relation between D_f and b holds for the GGF.

The rest of this paper is organized as follows. In the next section we describe the data that we analyze. Their analysis is described, discussed, and presented in Sec. III, where the data are utilized to estimate the fractal dimension of the fracture network of the GGF. In Sec. IV the parameter b of the GR law is evaluated for the microseismic events at the GGF, and its relation with D_f is studied. The implications of the resulting b and its relation with D_f are discussed in Sec. V. The paper is summarized in the last section.

II. THE DATA

We used the catalogs provided by the Lawrence Berkeley National Laboratory and the online data set from Northern California Earthquake Data Center [31]. The area covered by our study was the northwest (NW) region of the GGF, indicated by the rectangle in Fig. 1. As mentioned earlier, injection of cold water into the GGF induces microseismic events—earthquakes of small magnitudes. Their hypocenters and the locations of injection wells are shown in Fig. 2. Beall *et al.* [32] reported a strong correlation between seismic activity and the rate of injection of cold water into the NW region of the GGF. Based on the seismic activity of the area and the location of the injection wells, we initially defined three clusters that consisted of the spatial distributions of the hypocenters of the microseismic events; see Fig. 3. Cluster number 2, shown in Fig. 3, was then divided into four subclusters, and each of them was also analyzed to delineate the possible size effects. As Figs. 2 and 3 indicate, some clusters and subclusters are more dense than others. We deliberately selected such clusters in order to also understand the effect of the events' density on the properties computed.

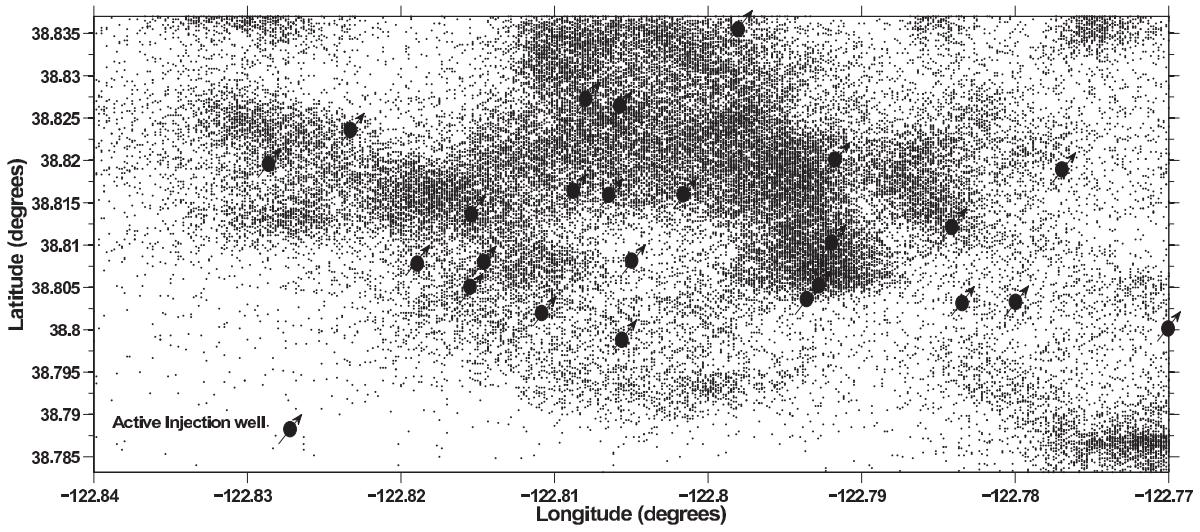

FIG. 2. Clusters of the earthquakes' hypocenters and the locations of active injection wells. Each point represents one event.

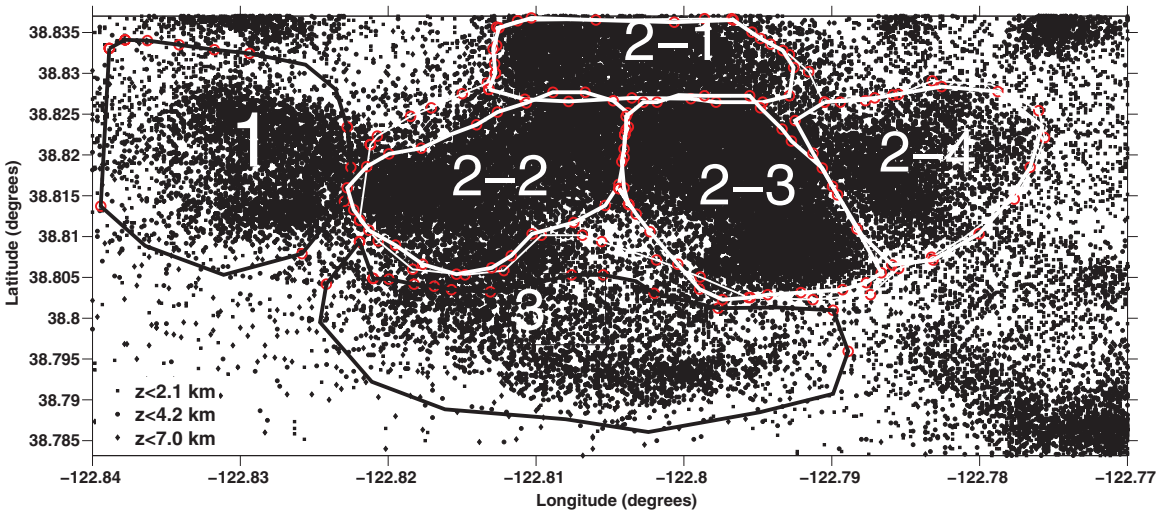

FIG. 3. (Color online) The four regions studied, as well as the four subregions. Each point represents the location of an event.

III. ANALYSIS OF THE DATA AND THE STRUCTURE OF THE FRACTURE NETWORK

The spatial distribution of the hypocenters of the seismic events in the clusters that are shown Fig. 3 was characterized by a fractal dimension D_f and the b value of the frequency-magnitude distribution, the GR law. The fractal dimensions were computed using the ZMAP program [33] that determines D_f using Eqs. (2) and (3). ZMAP is an interactive tool for investigating and visualizing seismicity as a function of space and time. It was originally designed to improve the resolution of potential seismicity anomalies, and to avoid the necessity of arbitrarily defining volumes for study, as well as to study the overall characteristics of earthquake catalogs. In particular, using ZMAP one can resolve seismicity rate changes as an almost continuous function of space and time, as well as carrying out detailed analyses on selected regions. As an example, Fig. 4 presents a plot of $\log C(r)$ for the entire spatial distribution of the hypocenters in region 2 of Fig. 3. The linear portion of the curve yields a fractal dimension, $D_f \simeq 2.59 \pm 0.02$. The interpretation of such values of D_f will be given shortly.

We should point out that the fractal dimension estimated from the data presented in Fig. 4 is for a bit less than two orders of magnitude variations in the distance r. In principle, the distance r over which the correlation function $C(r)$ is varied and used to estimate D_f must vary by about four orders of magnitude [34]. If the range of variations of r is not broad enough, then one must consider an alternative interpretation of the data [10,11]. Unfortunately, however, the range of length scales that can be explored in seismicity distributions is severely limited by the accuracy with which the individual events can be located, which itself is limited by the heterogeneity of the crust. At the same time, however, our data are not indicative of other interpretations and spatial distributions of the events. Thus, although one must, in principle, be cautious about attributing fractal characteristics to the data set and consider other possibilities, our results are completely consistent with such characteristics, as well as with the general expectations about the fractal character of the fracture network of rock.

Pickering *et al*. [35] suggested that in order to analyze more carefully the data for the two-point correlation function defined by Eqs. (2) and (3), one must "plot the local slope of the graphs and use this to determine the scale range or ranges over which the trend can be considered to approximate a straight line." If

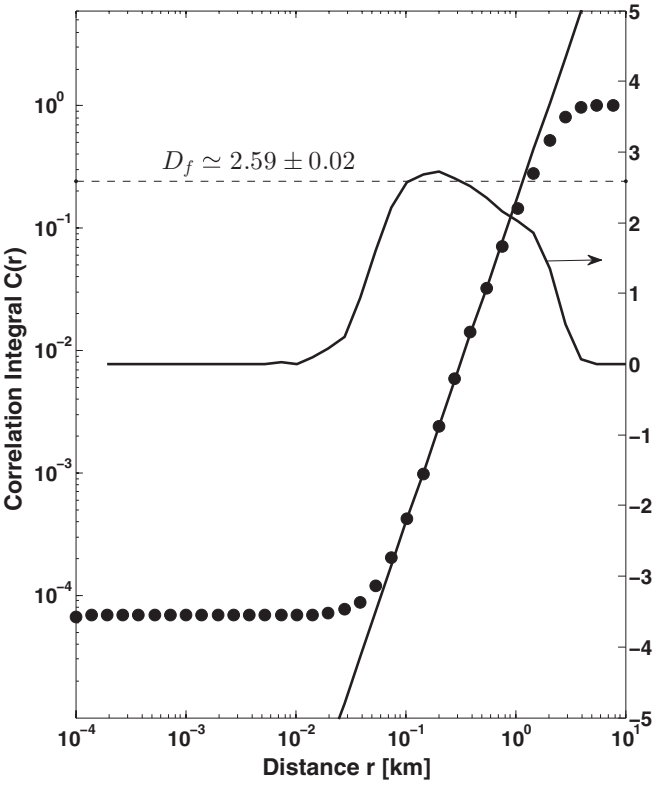

FIG. 4. The logarithmic plot of the correlation function $C(r)$ vs distance in region 2 of the Geysers geothermal field. Also shown are the variations of the local slopes around a constant value, indicating the accuracy of the data and the overall slope of the plot.

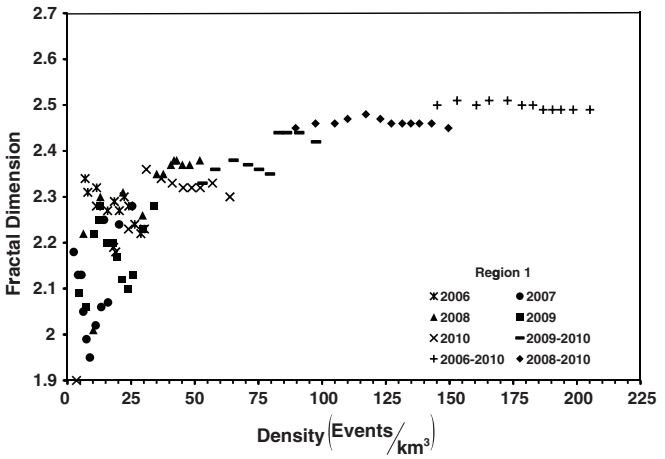

FIG. 5. Dependence of the fractal dimension D_f on the density of the microseismic events in region 1 from 2006 to 2010.

the variations of the local slopes are well-behaved and indicate a plateau, then a reliable estimate of the fractal dimension D_f can be obtained. In Fig. 4 we also show the variations of the local slope. It is zero over the tail region of $C(r)$ and rises where the power-law region begins. The scaling region where the power law is observed begins at $r \approx 0.04$ km. The local slope at that point is about 2.3. The maximum of the local slope is about 2.7, only 17% larger. At $r \approx 2$ km where the power-law region ends and $C(r)$ reaches a plateau, the local slope is about 2.1. The average of all the local slopes is 2.59. Hence, we conclude that the estimate of D_f from Fig. 4 is reliable.

Care is required in using seismicity to estimate the fractal dimension of a fracture network. Smith [36] and Robertson *et al.* [25] illustrated that there exists a minimum number of data points for estimating the true fractal dimension of the underlying fracture network. Eneva [37] also illustrated that the number of data points, the size of the region under study, and the measurements' error can significantly affect the estimate of the fractal dimension, and that assigning a specific physical meaning to the fractal dimension associated with a limited data set might be problematic. Thus, to ensure that we sampled a large enough number of data points in order to compute the true fractal dimension of the underlying fracture-fault network, the effective values of D_f were plotted as a function of the density of the events in a given cluster. Figure 5 presents the results for region 1, which demonstrates that the effective value of D_f converges to a constant value as the density of the events in the cluster increases. Figure 6 indicates the same trends for the fractal structure of the spatial distributions of the hypocenters in the four subregions carved out of region 2. For all the subregions, the fractal dimensions associated with the spatial distribution of the hypocenters converge to values that vary in a very narrow range. As a further test, the northwest region of the GGF was analyzed separately, with the results shown in Fig. 7, indicating again that the spatial distribution of the hypocenters in this region also forms a fractal cluster. All the estimated fractal dimensions are listed in Table I.

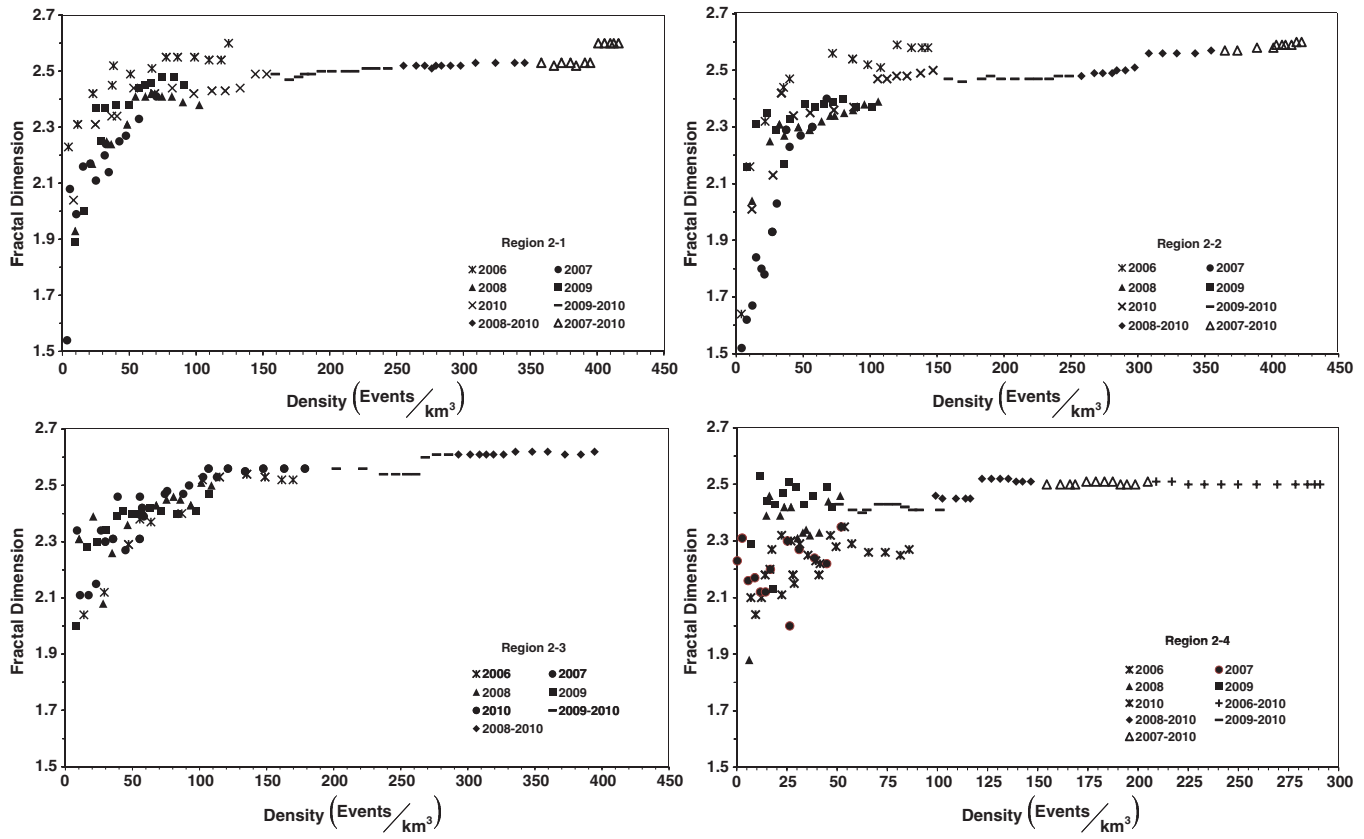

FIG. 6. Same as in Fig. 5, but for the four subregions carved out of region 2 from 2006–2010.

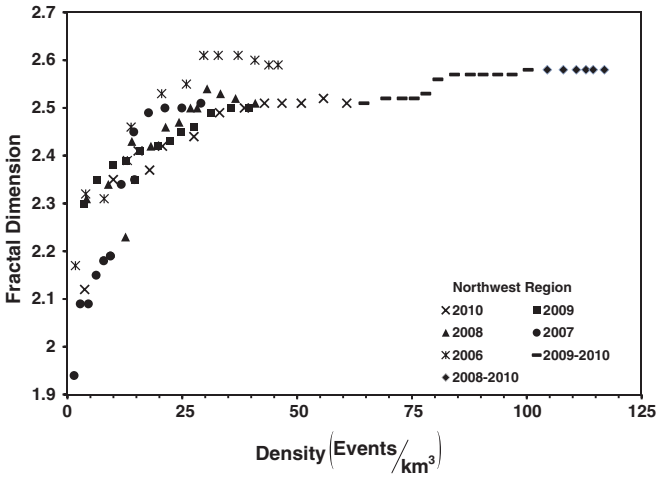

FIG. 7. Same as in Fig. 5, but for the northwest region, from 2006 to 2010.

When earthquakes are not induced by, for example, injection of cold water into a rock formation, and are of tectonic type, the value of D_f is always close to 2 [18]. Such a value of D_f has been interpreted in two different ways: One is that it indicates that most tectonic events occur on a subset of near-vertical faults, because they have lower normal stress. The second interpretation [18] is that the events occur on the fault network's *backbone*—its multiply connected part—which enables finite shear strain. The latter proposal is supported by the recent work of Pastén *et al.* [38], who analyzed the spatial distributions of hypo- and epicenters of earthquakes in central Chile and reported estimates of D_f that are consistent with this hypothesis. We shall come back to this point shortly.

In any case, estimates of D_f reported here are significantly larger than 2, hence confirming that seismic activity in the GGF is more likely to have been induced by the injection of cold water into the formation, rather than being of tectonic type. Therefore, the estimates of D_f provide significant insight into the structure of the fracture networks, as well as their *origin*. It is, therefore, possible to directly use the spatial distribution of microseismic events to map out the fracture network of a large-scale porous medium, such as geothermal reservoirs. In addition, the fact that computed D_f is significantly smaller than 3—the spatial dimension of the region in which the hypocenters are embedded—implies that only a small part of the overall structure contributes to distributing the strains.

TABLE I. Estimates of the fractal dimensions and the b values for the individual regions. Estimates of b are for the 2006–2010 period.

Region	Fractal dimension	b
NW region	2.58 ± 0.03	1.27 ± 0.02
Region 1	2.50 ± 0.03	1.33 ± 0.02
Region 2	2.63 ± 0.06	1.36 ± 0.02
Region 3	2.58 ± 0.03	1.28 ± 0.02
Region 2-1	2.60 ± 0.04	1.20 ± 0.05
Region 2-2	2.60 ± 0.04	1.10 ± 0.02
Region 2-3	2.62 ± 0.06	1.20 ± 0.03
Region 2-4	2.51 ± 0.03	1.17 ± 0.03

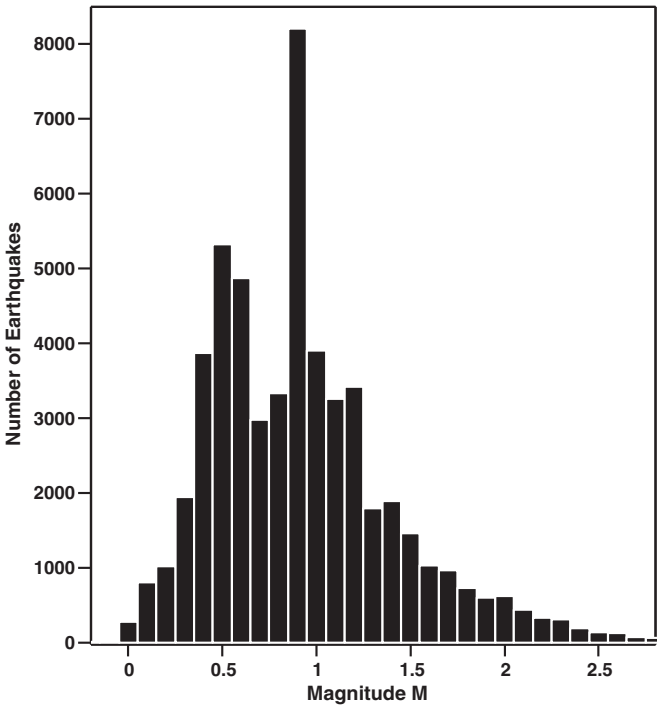

FIG. 8. Distribution of earthquakes' magnitudes in the Geysers geothermal field.

IV. THE b VALUES

The distributions of the magnitudes of the microseismic events are interesting and important. For example, Fig. 8 presents the distribution for the northwestern region of the GGF from 2006 to 2011. It peaks at $M \simeq 1$ but is not Gaussian (symmetric), as it has a relatively long tail for larger earthquakes. The same type of distribution was obtained for other regions of the GGF that we studied.

According to Eq. (4), b is the slope of the linear portion of the plot of $\log N$ versus M. The plot has negative curvature for small earthquakes, due to undersampling caused by the detection threshold. The break from negative curvature represents the so-called minimum magnitude of completeness, M_c. There is also deviation from linearity for large values of M, due to the limited observation times for properly sampling the much less frequent larger events. In most cases, M_c may be estimated by the maximum curvature method [39]. But, when we used the method, it did not yield physical estimates of b in some cases, in which case manual curve fitting was utilized for estimating the b values. If M_c is determined by the maximum curvature method, b is estimated using the maximum likelihood method, according to which

$$b = \frac{0.433}{\langle M \rangle - M_c}, \tag{5}$$

where $\langle M \rangle$ is the average magnitude of the earthquakes. A typical plot is shown in Fig. 9 for the northwestern region of the GGF during 2006, illustrating the application of the maximum likelihood method for estimating b.

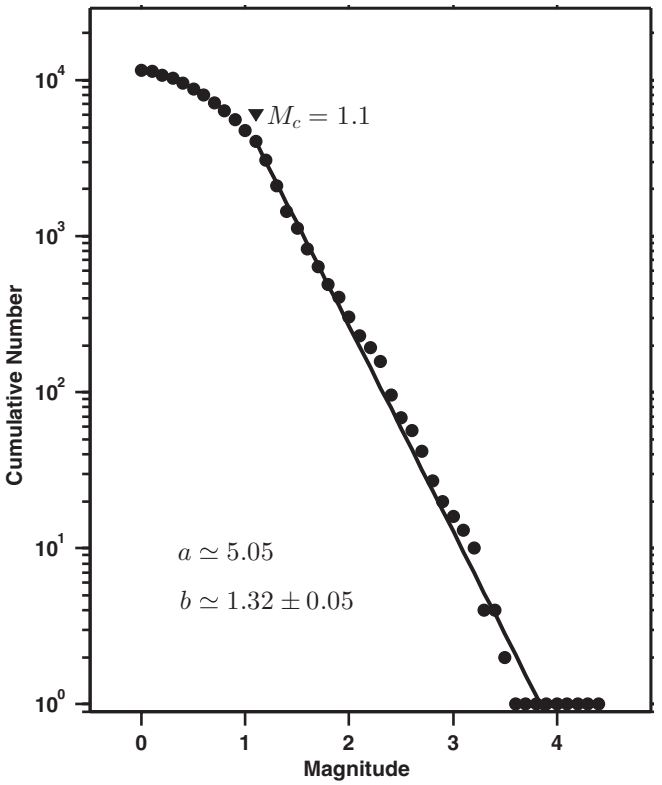

FIG. 9. The frequency-magnitude plot for extracting the b value for the entire seismicity catalog of the Geysers geothermal field.

But, more interesting are the variations of b over the time period in which we studied the microseismic events at the GGF. Figure 10 presents such variations for the four subregions studied. Except for region 3, the b values are all larger than 1.3, indicating the very large number of very small seismic events, as larger values of b correspond to smaller earthquakes, which explains why the b values that we obtain are all larger than 1, the typical value for large earthquakes with tectonic origin. More interestingly, the b values for the same three regions approach 1.2 and appear not to change for the next year or so between 2009 and 2010, and the nature of the events was still more likely to be of the induced type ($b > 1$) rather than the tectonic type ($b \approx 1$). These are all consistent with the catalog of the events that we studied. Wyss and Wiemer [39] emphasized the significance of studying the time variations of the b values.

Estimates of the b values vary from 1.11 to 1.32, and are all listed in Table I. They represent the estimates for the entire 2006–2010 period. As Table I indicates, values of b are more scattered than those of the fractal dimension D_f. This is, in fact, not surprising because although each hypocenter is on a fault, it is not obvious that each earthquake fully activates a fracture in the network, hence resulting in more uncertainty in the b values.

Note that, according to Table I, values of D_f and b for the three regions roughly follow the Aki relation, $D_f \approx 2b$, whereas those for the subregions do not. This is presumably due to the higher sensitivity of the b values to the size of the area in which seismic activity and microearthquakes occur. Note also that the estimates $b > 1$ confirm once again that the seismicity at the GGF is induced and does not have tectonic origin because, as pointed out earlier, the fractal dimension of the spatial distribution of earthquakes' hypocenters with a tectonic origin is usually close to 2 with a b value of about 1 [40]. It has been suggested by some [41] that high b values are a necessary, but not sufficient, condition for the earthquakes

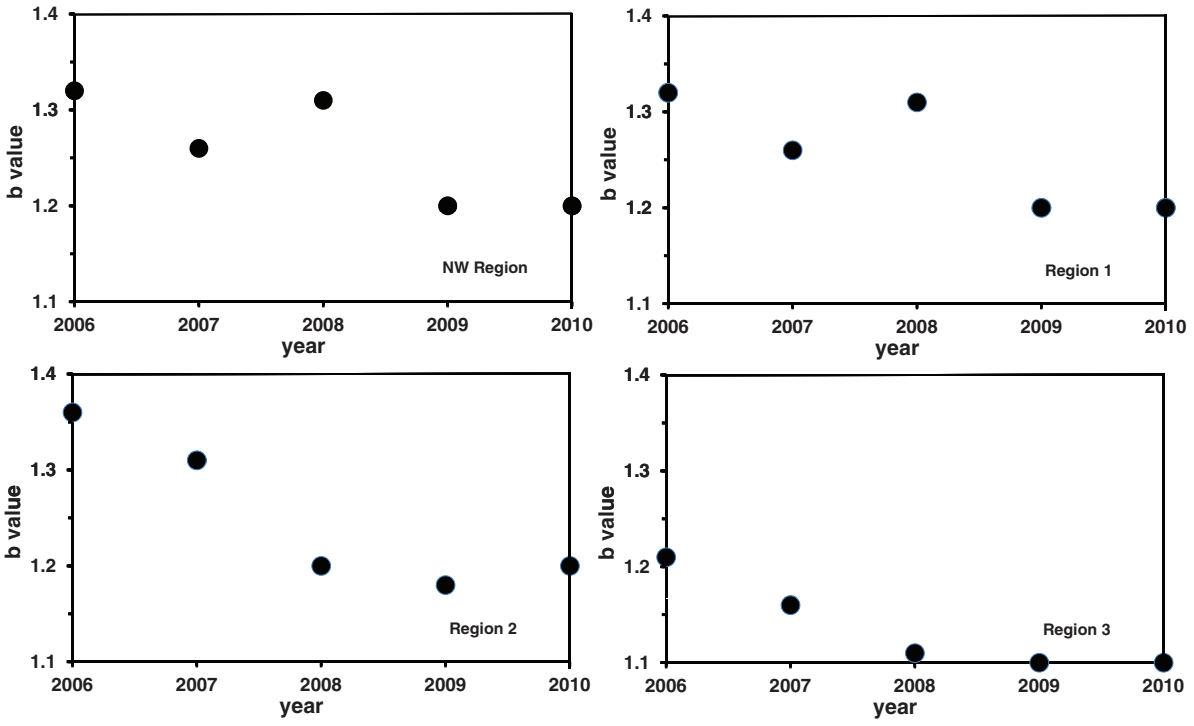

FIG. 10. Time dependence of the b values in the four regions of the Geysers geothermal field.

to occur near an active magmatic body, but the hypothesis is not applicable to the GGF. We also emphasize that, at this point, we are only documenting our findings for the GGF, and provide a plausible explanation. Clearly, much work needs to be done to check the generality of the proposal. See Refs. [42-44] for alternative interpretations and discussions.

V. IMPLICATIONS OF THE RESULTS

If fractures nucleate and grow more or less at random in a highly heterogeneous medium, such as large-scale porous formations, then they should form a network of interconnected fractures that resembles a percolation cluster [45,46], i.e., a cluster of (more or less) randomly distributed interconnected fractures that percolate between two widely separated planes. To put this on a more intuitive but physically understandable basis, we appeal to the critical path analysis (CPA) first developed by Ambegaokar *et al*. [47] and confirmed by many sets of simulations. They argued that transport processes in a highly heterogeneous medium can be reduced to one in a percolation system at or very near the percolation threshold. The idea is that in a medium with broadly distributed heterogeneities, a finite portion of the system possesses a very small conductivity, hence making a negligible contribution to the overall conductivity or other effective flow or transport properties. Therefore, zones of low conductivity may be eliminated from the medium, which would then reduce it to a percolation system. Ambegaokar *et al*. [47] described a procedure by which the equivalent percolation network, called the critical path, is built up, and they showed that the resulting percolation system is at or very near its percolation threshold.

When applied to heterogeneous fractured rock [10], the CPA implies that the fracture network must have the connectivity of a percolation cluster because, for example, the fractures are the main conduits for fluid flow in rock as their permeabilities or hydraulic conductances are much larger than those of the matrix in which they are embedded. Using the procedure of Ambegaokar *et al*. [47], one then finds that the fracture network of rock must be at, or very near, its percolation threshold.

The relationship between percolation theory, the spatial distribution of earthquakes' hypo- and epicenters, and the fault-fracture networks was first explored by Otsuka and others [48] in a qualitative manner, but was put on a quantitative foundation by Sahimi *et al*. [18]. The utility of identifying the fracture network of large-scale porous media with the sample-spanning percolation cluster is that the latter has been studied extensively [45,46]. In particular, it is well known that the sample-spanning percolation cluster at or very near the percolation threshold is a self-similar fractal object with a fractal dimension, $D_f \simeq 1.9$ and 2.53, in two and three dimensions, respectively. Moreover, the multiply connected part of the cluster, which allows various phenomena such as fluid flow and stress transport to occur in the network, is the aforementioned backbone, which is also a fractal object with fractal dimensions of 1.64 and 1.9 in two and three dimensions, respectively. Indeed, as mentioned earlier, the recent work of Pastén *et al*. [38], who analyzed the spatial distributions of hypo- and epicenters of earthquakes in central Chile, yielded $D_f \simeq 2.02 \pm 0.05$ and 1.73 ± 0.02, respectively, which are within 5% of the fractal dimensions of 3D and 2D percolation backbones.

We must point out that a network of interconnected fractures and/or faults with irregular shapes and sizes resembles what is usually referred to as *continuum percolation* [49], which differs from the better known and more studied lattice percolation that deals with networks of bonds and sites. All the numerical and analytical works have indicated [49], however, that the fractal dimensions of the sample-spanning clusters and their backbone are the same for lattice and continuum percolation.

The estimates of the fractal dimensions listed in Table I deviate from that of the sample-spanning percolation cluster by at most 4%, well within the estimated errors, but they are not close to that of the percolation backbone. Thus, the seismicity induced by the injection of cold water happens on a fracture network that is similar to the 3D sample-spanning percolation cluster, whereas the tectonic events occur on the backbone of the fault network. The reason is that when cold water is injected into GGF, the path that the fluid takes within the porous formation and the fractures that it generates within the rock are, due to the heterogeneity of the formation, random. Even if the path is not random but contains extended correlations, the structure of the cluster at the largest length scale should still resemble that of a percolation cluster. The high-pressure cold water generates some fractures that are dead-ends, because the growth of such fractures stops only when the pressure of the water cannot overcome the resistance offered by the rock. As a result, the network generated by the injection contains both dead-end as well as multiply connected fractures, i.e., the sample-spanning percolation cluster.

On the other hand, for earthquakes of tectonic origin to occur, finite strains and deformations must occur on the fault or fracture network. But that is possible only on the multiply connected part of the cluster, as the singly connected faults or fractures are dead-ends and cannot contribute to strain release. Therefore, such earthquakes should occur on the backbone of the fault-fracture network, which has a much lower fractal dimension, close to 2.

The significance of the link between the structure of a fracture network and those of percolation clusters and their backbones is that the latter have been studied extensively, and deep insights into their structural properties have been gained [45,46]. The relationship between D_f and the b values opens up another path for characterization of a fracture network of highly heterogeneous rock. The knowledge can, therefore, be used for realistic modeling of a fracture network of the GGF, or that of any other rock formation for that matter.

VI. SUMMARY

We analyzed the structure of the spatial distribution of hypocenters of microseismic events in Geysers geothermal field. The results indicate that the distribution forms a fractal cluster with a fractal dimension that is very close to that of a 3D sample-spanning percolation cluster. The results also indicate that the spatial locations of microearthquakes' hypocenters provide deeper insight into the structure of the fracture network

of large-scale porous media. Furthermore, the correlation between the fractal dimension of the fracture network and the parameter b in the Gutenberg-Richter frequency-magnitude distribution was investigated. The results indicate that if the size of the region under study is large enough, the Aki relation, $D_f = 2b$, is satisfied, at least to a very good degree of approximation. Together, D_f and b provide insight into the physical origin of the fracture network of the GGF, and quite possibly any other rock formation.

We emphasize that we make no claim to have provided a general proof of the Aki conjecture for all types of fractured rock, or even that our results are general and applicable to all microseismic events. What we do offer is a plausible explanation as to why both b and D_f may be expected to be high in geothermal reservoirs, and any other pressurized environment for that matter. More work is required to test the generality of our results.

There have been several recent reports (see, for example, Ref. [50]) that hydraulic fracturing—so-called *fracking*—can cause earthquakes. The work presented in this paper not only lends support to this possibility, but also provides a tool for using the data to gain information and insight into the structure of the fracture network, and to show that it is indeed fracking that generates the fracture network. Therefore, more study is called for in this important and emerging area of research.

ACKNOWLEDGMENTS

This work was supported by the Department of Energy. The authors would like to thank the Northern California Earthquake Data Center and Lawrence Berkeley National Laboratory for providing catalogs of microseismic events at the Geysers geothermal field. We are grateful to Joseph Beall and Mark Walter from Calpine for their advice and support.

[1] M. Wyss, Geophys. J. R. Astron. Soc. **31**, 341 (1973).
[2] J. Hebein, in *Proceedings of the 11th Stanford Workshop on Geothermal Reservoir Engineering* (Stanford University Press, Stanford, CA, 1986), pp. 43–50.
[3] J. Sternfeld, Trans. Geotherm. Resour. Counc. **13**, 473 (1989).
[4] C. G. Sammis, L. J. An, and I. Ershaghi, in *Proceedings of the 16th Workshop on Geothermal Reservoir Engineering* (Stanford University Press, Stanford, CA, 1991).
[5] D. Nielson, M. Walters, and J. Hulen, Trans. Geotherm. Resour. Counc. **15**, 27 (1991).
[6] M. Lou, E. Shalev, and P. Malin, Geophys. Res. Lett. **24**, 1895 (1997).
[7] P. Malin and E. Shalev, in *Proceedings of the 24th Stanford Workshop on Geothermal Reservoir Engineering* (Stanford University Press, Stanford, CA, 1999).
[8] D. Erten, M. Elkibbi, and J. Rial, in *Proceedings of the 26th Workshop on Geothermal Reservoir Engineering* (Stanford University Press, Stanford, CA, 2001), pp. 139–147.
[9] M. Elkibbi, M. Yang, and J. Rial, Trans. Geotherm. Resour. Counc. **28**, 789 (2004).
[10] M. Sahimi, *Flow and Transport in Porous Media and Fractured Rock*, 2nd ed. (Wiley-VCH, Weinheim, 2011), Chap. 6.
[11] E. Bonnet, O. Bour, N. E. Odling, P. Davy, I. Main, P. Cowie, and B. Berkowitz, Rev. Geophys. **39**, 347 (2001).
[12] C. C. Barton, and E. Larsen, in *Proceedings of the International Symposium on Fundamentals of Rock Joints*, edited by O. Stephansson (Bjorkliden, Sweden, 1985), p. 77; C. C. Barton, T. A. Schutter, W. R. Page, and J. K. Samuel, Trans. Am. Geophys. Union **68**, 1295 (1987); C. C. Barton and P. A. Hsieh, *Physical and Hydrological-Flow Properties of Fractures, Guidebook T385* (American Geophysical Union, Las Vegas, 1989).
[13] P. LaPointe, Int. J. Rock Mech. Min. **25**, 421 (1988).
[14] B. Velde, J. Dubois, D. Moore, and G. Touchard, Earth Planet. Sci. Lett. **104**, 25 (1991).
[15] M. Vignes-Adler, A. Le Page, and P. M. Adler, Tectonophysics **196**, 69 (1991).
[16] C. C. Barton, in *Fractals and Their Use in the Earth Sciences*, edited by C. C. Barton and P. R. LaPointe (Geological Society of America, Washington, DC, 1992); see also C. C. Barton, *Bedrock Geological Map of Hubbard Brooks Experimental Forest and Maps of Fracture and Geology in Road Cuts along Interstate 93, Grafton County, New Hampshire*, *Rep. I-2562*, US Geological Survey Misc. Invest. Ser. 2, 1 (1995).
[17] C. G. Sammis, L. J. An, and I. Ershaghi, in *Proceedings of 17th Stanford Workshop on Geothermal Reservoir Engineering* (University of Southern California, Los Angeles, California, 1992), pp. 79–85.
[18] M. Sahimi, M. C. Robertson, and C. G. Sammis, Phys. Rev. Lett. **70**, 2186 (1993); H. Nakanishi, M. Sahimi, M. C. Robertson, C. G. Sammis, and M. D. Rintoul, J. Phys. I **3**, 733 (1993).
[19] C. G. Hatton, I. G. Main, and P. G. Meredith, J. Struct. Geol. **15**, 1485 (1993).
[20] T. Hirata, T. Satoh, and K. Ito, Geophysics **90**, 369 (1987).
[21] M. Sahimi and J. D. Goddard, Phys. Rev. B **33**, 7848 (1986); L. de Arcangelis, A. Hansen, H. J. Herrmann, and S. Roux, *ibid.* **40**, 877 (1989); S. Arbabi and M. Sahimi, *ibid.* **41**, 772 (1990); M. Sahimi and S. Arbabi, *ibid.* **47**, 713 (1993).
[22] M. Sahimi and S. Arbabi, Phys. Rev. Lett. **68**, 608 (1992); **77**, 3689 (1996).
[23] M. Sahimi, *Heterogeneous Materials II* (Springer, New York, 2003), Chap. 7.
[24] H. J. Herrmann, M. Sahimi, and F. Tzschichholz, Fractals **1**, 795 (1993).
[25] T. Hirata, J. Geophys. Res. B **94**, 7507 (1989).
[26] M. C. Robertson, C. G. Sammis, M. Sahimi, and A. J. Martin, J. Geophys. Res. B **100**, 609 (1995).
[27] K. Aki, in *Earthquake Prediction: An International Review*, edited by D. Simpson and P. Richards (American Geophysical Union, Washington, D.C., 1981), p. 566.
[28] H. Kanamori and D. Anderson, Bull. Seism. Soc. Am. **65**, 1073 (1975).
[29] M. Wyss, C. G. Sammis, R. M. Nadeau, and S. Wiemer, Bull. Seism. Soc. Am. **94**, 410 (2004).
[30] C.-C. Chen, W.-C. Wang, Y.-F. Chang, Y.-M. Wu, and Y.-H. Lee, Geophys. J. Int. **167**, 1215 (2006).
[31] See http://www.ncedc.org/SeismiQuery/events_f.html.

[32] J. J. Beall, M. C. Wright, A. S. Pingol, and P. Atkinson, Trans. Geotherm. Resour. Counc. **34**, 1203 (2010).
[33] See http://www.earthquake.ethz.ch/software/zmap; see also http://www.geociencias.unam.mx/∼ramon/ZMAP/intro.html.
[34] P. Grassberger and I. Procaccia, Physica D **9**, 189 (1983).
[35] G. Pickering, J. M. Bull, and D. J. Sanderson, Tectonophysics **248**, 1 (1995).
[36] L. Smith, Phys. Lett. A **133**, 283 (1988).
[37] M. Eneva, Geophys. J. Int. **124**, 773 (1996).
[38] D. Pastén, V. Muñoz, A. Cisternas, J. Rogan, and J. A. Valdivia, Phys. Rev. E **84**, 066123 (2011).
[39] M. Wyss and S. Wiemer, Science **290**, 1334 (2000).
[40] C. Frohlich and S. D. Davis, J. Geophys. Res. B **98**, 631 (1993).
[41] S. Wiemer, S. R. McNutt, and M. Wyss, Geophys. J. Int. **134**, 409 (1998).
[42] I. G. Main, Geophys. J. Int. **111**, 531 (1992).
[43] J. Henderson, I. G. Main, R. Pearce, and M. Takaya, Geophys. J. Int. **116**, 217 (1994).
[44] A. O. Öncel, I. G. Main, Ó. Alptekin, and P. A. Cowie, Tectonophysics **257**, 189 (1996).
[45] D. Stauffer and A. Aharony, *Introduction to Percolation Theory*, 2nd. ed. (Taylor & Francis, London, 1994).
[46] M. Sahimi, *Applications of Percolation Theory* (Taylor & Francis, London, 1994).
[47] V. Ambegaokar, B. I. Halperin, and J. S. Langer, Phys. Rev. B **4**, 2612 (1971); see also A. Hunt and R. Ewing, *Percolation Theory for Flow in Porous Media*, 2nd ed. (Springer, Berlin, 2009) for a clear discussion of the CPA.
[48] M. Otsuka, Butsuri-Tansa **34**, 509 (1979); T. Chelidze, Dokl. Akad. Nauk USSR **246**, 14 (1981); C.-I. Trifu and M. Radulian, Phys. Earth Plant. Interiors **58**, 277 (1989); C. P. Stark and J. A. Stark, J. Geophys. Res. B **96**, 8417 (1991).
[49] I. Balberg, in *Encyclopedia of Complexity and System Science*, edited by R. A. Meyers (Springer, New York, 2009), Vol. 2, p. 1443.
[50] See, for example, http://www.ecocentricblog.org/2012/04/11/fracking-operations-can-cause-earthquakes-“almost-certainly”-says-u-s-geological-survey.